JOURNAL OF CATALYSIS 140, 497–509 (1993)

Relationship between the Scaling of the Acid Strength of Lewis Sites by EPR and NMR Probes

D. J. COSTER, A. BENDADA, F. R. CHEN, AND J. J. FRIPIAT[1]

Department of Chemistry and Laboratory for Surface Studies, University of Wisconsin–Milwaukee, Milwaukee, Wisconsin 53201

Received June 4, 1992; revised November 12, 1992

While numerous techniques have been successful for scaling the acid strength of Brønsted sites, the situation is not satisfactory at all, for the Lewis acid sites. This is most unfortunate, since Lewis sites are present in most acid catalysts. This contribution aims to show that the simultaneous use of EPR and NMR probes suggests solutions to the problem of scaling the acid strength of Lewis sites. As shown previously, the hyperfine splitting of the EPR spectrum of the aniline radical cation or of the O_2^- superoxide ion is a measurement of the strength of the electron acceptor site. Other researchers have suggested the shielding of the ^{31}P nucleus and the shift of its resonance lines in chemisorbed trimethylphosphine (TMP) as a measurement of the Lewis acid strength. The comparison of the scaling obtained on a set of superacids, namely, and in the decreasing order of acidity, the sulfated derivatives of ZrO_2, HfO_2, Al_2O_3 and TiO_2, by either the EPR or the NMR probes gives interesting information. While very strong Lewis acid centers in sulfated ZrO_2 and HfO_2 are revealed by ^{31}P downfield shifted resonance lines, no such lines are observed in sulfated Al_2O_3 or TiO_2 or zeolites (such as dealuminated mordenite) which contains strong Lewis acid centers. In the latter samples, the most downfield shifted line corresponds to that generally assigned to $TMPH^+$. Measurement of ^{31}P relaxation rates suggests that TMP has a more restricted mobility on strong than on weak Lewis sites. They also show that the origin of the relaxation in $TMPH^+$ is ambiguous: either the mobility of $TMPH^+$ is very restricted and/or the extraproton is not as close to the phosphorus as anticipated. © 1993 Academic Press, Inc.

INTRODUCTION

Scaling the strength of acid sites has always been a subject of interest in catalysis. Whereas spectroscopic techniques such as the infrared study of adsorbed pyridine are routinely carried out to differentiate Brønsted from Lewis sites, the measurement of the strength of Brønsted sites is still an active domain of research. Weakly basic Hammett indicators have been used in the past and are still used to characterize Brønsted sites in solid acids, and new developments are published regularly (*1*). The proton transfer to a proton acceptor molecule can also be studied by NMR and there have been numerous studies on that aspect: just to list and comment on them would be outside the scope of this communication.

When it comes to Lewis acids, the situation is more confusing because the measurement of fractional electron transfer between a Lewis base and the acid center is not straightforward. In the 1960s, a great deal of attention was drawn to the use of EPR to characterize the formation of radicals, such as in the pioneering work of Stamires and Turkevich (*2*) and W. K. Hall (*3*). The advantage and inconvenience of EPR are notorious: very high sensitivity and too high a sensitivity! Indeed, this technique can pick up such weak signals that it is sometimes difficult to evidence the centers, which actually play a role in Lewis acidity. Probably, the measurement of the hyperfine structure of radicals contains the most reliable information, since it is a measurement of the

[1] To whom correspondence should be addressed.

0021-9517/93 $5.00

extent of electron delocalization. This old idea was reactivated recently by Chen and Fripiat (*4*), who studied H-mordenite and H-Y containing nonframework aluminum. Molecular oxygen adsorbed after (H-mordenite) or during (H-Y) the adsorption of aniline forms the superoxide ion O_2^- which interacts with one ^{27}Al nucleus, as evidenced by the superhyperfine structure of a simple six-line set. Moreover, the value of the superhyperfine splitting of O_2^- seems to reflect the strength of the electron acceptor site. New developments along this line of thought are in progress (*5*). Thus, the hyperfine splitting can be obtained from the g_{zz} component of the g tensor. The rationale underlying the claim that the value of the A_{zz} splitting is related to the acid strength of the electron acceptor center relies on the demonstrated relationship between the hyperfine splitting constant and the spin density on the nucleus which causes the splitting (*6*). For instance, the largest A_{zz} will correspond to the highest electron density on the Al center, namely, that with the highest electron affinity. However, there are several additional factors which can affect this simple relationship. One is the environment of the Al center (*7*) and the electron–Al distance is another. Thus, the scaling of the Lewis acid strength using the hyperfine splitting of O_2^- is not straightforward. In such a situation, a safe approach would be to measure hyperfine splittings on a set of Lewis acids of known strength. For instance, the aniline radical cation itself shows hyperfine splitting due to the interaction of the electron with the nitrogen nucleus ($I = 1$) and the two equivalent hydrogen nuclei ($I = \frac{1}{2}$), and the width of the nine-line spectrum should decrease with increasing strength of the electron-accepting center (*5*). This is an alternative possibility for the cases where the O_2^- hyperfine splitting is not measureable. Thus, the use of an EPR molecular probe for scaling the Lewis acid strength has its own limitation.

An alternative way is in using in parallel another technique. We have selected the ^{31}P NMR resonance of $P(CH_3)_3$ (TMP) for this goal. The research groups of Lunsford (*8, 9, 11*) and Maciel (*10*) have demonstrated the versatility in this technique. $(CH_3)_3P$: is, indeed, a weak Lewis base which interacts with an acid surface in forming the $(CH_3)_3PH^+$ adduct on Brønsted sites and $(CH_3)_3P$:L, L, representing Lewis sites. The deshielding of the ^{31}P nucleus increases with the extent of the electron transfer which shifts the ^{31}P resonance downfield with respect to physically adsorbed TMP.

It remains the critical choice of a set of superacids whose strengths are known, at least approximately. For that purpose we took the set of sulfate-supported TiO_2, ZrO_2, HfO_2, SnO_2, and Al_2O_3 reviewed by Kazuski Arata (*13*). It is important to emphasize that from IR study, these solids contain Brønsted *and* Lewis acids. In fact, the Lewis acidity is probably created by the electron withdrawal power of SO_4 on the neighbor metallic cation, while the Brønsted acid would come from chemisorbed water on the Lewis site. In our opinion, the coexistence of both kinds of acid sites shed a doubt on the significance of the measurement of acid strengths of these solids with Hammett indicators, since in both cases, the Hammett acidity function H_0

$$H_0 = pK_a + \log\frac{[B]}{[AB]}$$

is a function of the pK_a and of the concentration ratio of the neutral base $[B]$ and of its acid adduct $[AB]$, where A is either the proton or the Lewis site. In fact, Arata gives acid strengths obtained from Hammett indicators without explicit reference to the nature of B. From such a series of measurements, the acid strengths scaling is the following for the aforementioned sulfated oxides, $ZrO_2 \geq SnO_2 > TiO_2 \simeq Al_2O_3$ under the most adequate preparation procedures. From catalytic performances (butane isomerization) Arata reported that HfO_2–SO_4 should be as strong an acid as ZrO_2–SO_4.

Thus, the first goal of this contribution is to compare the information obtained using EPR molecular probes (aniline and O_2) and

the NMR probe $(CH_3)_3P$ on superacids. Thereafter, the same techniques will be applied to dealuminated or steamed zeolites (with appreciable amounts of nonframework aluminum) and to aluminas. Aluminas rich or poor in pentacoordinated aluminum (*14*) were chosen for that purpose. These samples are of interest because alumina moieties in zeolites show the characteristic resonance due to this unusual Al coordination (Al^V), besides the expected resonances attributable to fourfold (Al^{IV}) and sixfold (Al^{VI}) coordination.

EXPERIMENTAL

Materials

The SO_4-supported ZrO_2, HfO_2, SnO_2, Al_2O_3, and TiO_2 were prepared as reviewed in Ref. (*13*). More specifically, the preparations were carried on as follows. $Zr(OH)_4$ and $Hf(OH)_4$ were prepared from $ZrOCl_2$ and $HfCl_4$, respectively. Aqueous ammonia (28%) was added slowly into a 0.4 *M* solution of $ZrOCl_2$ or $HfCl_4$ at room temperature until pH 9. $Ti(OH)_4$ was obtained with $TiCl_4$ and $Ti[OCH(CH_3)_2]_4$ as starting material. Two solutions were prepared, one by slowly adding 145 ml of $Ti[OCH(CH_3)_2]_4$ into 1 liter of distilled water at room temperature (the white precipitate formed was dissolved by gradually adding concentrated HNO_3) and the other by slowly adding 40 ml of $TiCl_4$ into 1 liter of distilled water. Aqueous ammonia was slowly added to the two solutions until pH 8 to form the gels. $Sn(OH)_4$ was obtained by hydrolyzing 100 g of $SnCl_4 \cdot xH_2O$ dissolved in 1 liter of water with aqueous ammonia until pH 9.7. The gels were then washed with distilled water until no Cl^- could be detected, and dried at 70°C overnight. The ZrO_2–SO_4, HfO_2–SO_4, and TiO_2–SO_4 were obtained by treating the corresponding metal hydroxide with 0.1 *M* H_2SO_4 solution (30 ml per 2 g of solid) for 20 min followed by filtration, drying overnight at 70°C and calcination for 4 h in air at 550°C or 650°C, 700°C, and 500°C, respectively. One sample TiO_2–SO_4 was calcined at 350°C.

The SnO_2–SO_4 was prepared by treating $Sn(OH)_4$ in 3 *M* H_2SO_4 solution for 20 min followed by filtration, drying, and calcination in air for 4 h at 500°C.

The Al_2O_3–SO_4 was obtained by treating an aluminum hydroxide gel calcined at 700°C for 5 h by 2.5 *M* H_2SO_4 followed by filtration, drying, and calcination at 600°C for 4 h in air. The gel was prepared by aging 1 *M* $AlNO_3$ at pH 12 and 60°C for 24 h, and then washed and dried at 70°C overnight. The same preparation was used on γ-alumina, but the results were the same as those obtained on the gel.

The preparation of the alumina catalysts has been described in Ref. (14), while that of the zeolites can be found in Refs. (*4*) and (*5*). From ^{29}Si NMR we obtained the following $[Si/Al^{IV}(F)]$ ratios: HY 650: 13.7 ± 0.6 after dealumination and steaming, while upon steaming HY at 650°C it is 11. This ratio is 32 for dealuminated HM heated at 550°C. HL was prepared as indicated in Ref. (*5*). The $[Si/Al^{IV}(F)]$ ratio was 4.9.

Techniques

The EPR techniques have been described thoroughly in Refs. (*4*) and (*14*).

The ^{31}P NMR experiments were carried out essentially as originally described by Lunsford and co-workers (*8*). TMP was obtained through thermal decomposition of the AgI complex, distilled under vacuum, and kept dried on a molecular sieve in an all-glass instrument fitted with greaseless stopcocks. To this instrument small glass ampules containing the samples were sealed. They were outgassed overnight at 450°C and treated eventually for a few hours with O_2 at the same temperature and outgassed again. The temperature was lowered to 80°C and about 20 torr TMP were introduced and let in contact with the sample for about 1 h. Afterwards, TMP was outgassed at 80°C for 1 h. The small ampules were sealed in a special lathe allowing a perfect alignment of the glass seal on their rotation axis. These ampules fit a DOTY 7-mm MAS probe where they can be spun easily up to 5 kHz.

In order to distinguish the spinning side bands (SSB) from the $-\frac{1}{2} \rightarrow +\frac{1}{2}$ transition, the ^{31}P resonance line(s) were recorded under magic angle spinning at least at two spinning rates. From the best fit of a spectrum simulation to the recorded spectrum, the distinction between SSB and transitions was relatively easy. The resonance frequency was 202 MHz and the 90° pulse width was about 5 μs. The delay time between acquisitions was 1 s and several thousand acquisitions were recorded. The chemical shift is expressed with respect to an 85% H_3PO_4 standard. The probe used for this work does not permit proton decoupling or proton cross-polarization. In a few cases spectra were recorded at temperature between +25 and −43°C. ^{31}P longitudinal relaxation times, T_1, were measured at room temperature by the saturation recovery method, the length of the pulse being adjusted in each case for maximum magnetization.

Now, it is appropriate to compare briefly the sensitivity of the EPR and of the NMR techniques. An objection could be that the observation of the ^{31}P resonance may miss what the EPR probes reveal. The number of aniline radical cations detected on the dealuminated mordenite was in the order of 10^{18} spins g^{-1}, as was the number of superoxide O_2^- ions observable in zeolites (*4*). On the Al^V rich alumina these figures were about 0.4×10^{18} spins g^{-1} (*14*). Absolute intensity measurements of the ^{31}P resonance line were performed on mixtures of $(NH_4)H_2PO_4$ and $NaNO_3$ (linewidth ~0.6 kHz) in decreasing proportion. It was found that upon accumulating 3000 scans, 10^{18} ^{31}P spins per g gave a strong line with S/N ratio better than 10. Thus, under the condition that the ^{31}P line does not become too broad, it may be claimed that both the EPR and NMR probes have, in the cases described here, comparable sensitivities.

RESULTS

Scaling the Acid Strength of the Superacids

Aniline was the EPR probe molecule and the overall width of the radical cation ($R^{+\cdot}$) spectrum yields the desired information. Figure 1 shows typical EPR spectra obtained for ZrO_2–SO_4, HfO_2–SO_4, and Al_2O_3–SO_4. Their widths are 36.5, 38.5, and 47.7 g, respectively, indicating that ZrO_2–SO_4, indeed, is the strongest and Al_2O_3–SO_4 the weakest acid in this series. TiO_2–SO_4 and SnO_2–SO_4 produce observable signals probably attributable to $R^{+\cdot}$, but without hyperfine structure. Paramagnetic centers are observed before aniline adsorption on ZrO_2–SO_4 and HfO_2–SO_4, with the following g values: ZrO_2–SO_4: $g_\perp = 1.979$, $g_\parallel = 1.951$; HfO_2–SO_4: $g_\perp = 1.973$, $g_\parallel \simeq 1.935$. These signals do not overlap with $R^{+\cdot}$ signal. Figure 2 shows the ^{31}P spectra obtained for ZrO_2–SO_4 and Al_2O_3–SO_4. Beside the spinning side bands (SSB), indicated by stars, ^{31}P on ZrO_2–SO_4 has four distinct resonances at 26, 23, −3.2, and −33 ppm, the latter being overlapped by SSB. It is only by recording spectra at different spinning rates and using simulation that the −33-ppm resonance can be evidenced without ambiguity. On Al_2O_3–SO_4, two resonance lines are easily observed at −4 ppm and −46 ppm. The lines at +26 and +23 ppm on ZrO_2–SO_4 and that at −46 ppm on Al_2O_3–SO_4 correspond to the most deshielded and to the most shielded ^{31}P resonances observed for the superacids. According to Refs. (*8*, *11*), a line at about −4 ppm has to be assigned to the $(CH_3)_3PH^+$ adduct, indicating Brønsted sites. Note, however, the width of the line at −4 ppm observed for Al_2O_3–SO_4 as opposed to the narrowness of the line at −3.3 ppm on ZrO_2–SO_4.

Table 1 summarizes the experimental NMR and EPR data. The adsorption of TMP on SnO_2–SO_4 produced a very broad (~100 ppm) featureless band, for unknown reasons. Accordingly, the aniline radical cation yielded a featureless line. TiO_2, which is also the weakest among the superacids shows a detectable ^{31}P line with downfield shift at −3.7 ppm only for the sample calcined at 350°C.

The Brønsted sites giving the $(CH_3)_3PH^+$ adduct in the superacid are probably formed

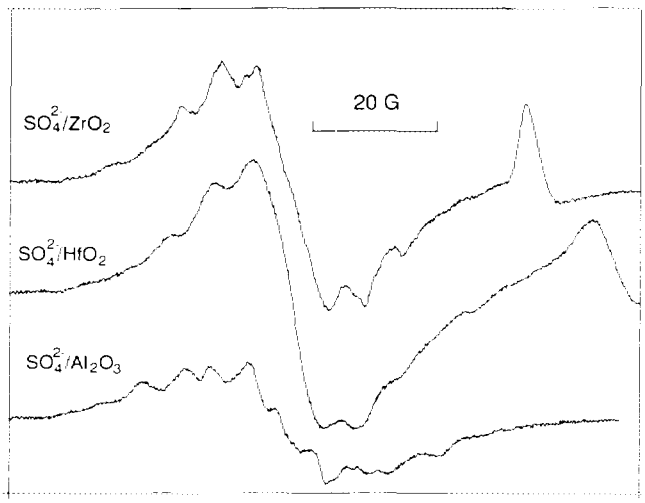

FIG. 1. EPR spectra of aniline radical cation formed on superacids. Ordinate: intensity (a.u). The lines at the right side are those of the bare support.

by chemisorption of water on L (Lewis) sites. Therefore, the amount of water saturating these sites may vary depending upon the outgassing temperature. This is particularly evident for TiO_2–SO_4, since calcination above 500°C suppresses the line ca. −4 ppm. However, some contribution of SOH acid groups cannot be ruled out.

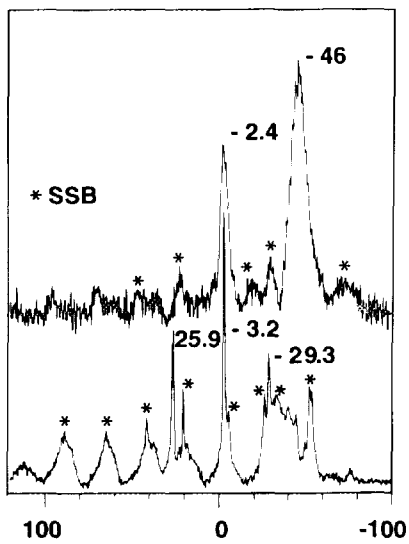

FIG. 2. ^{31}P single-pulse MAS NMR spectrum of TMP chemisorbed (bottom) on ZrO_2–SO_4; (top) on Al_2O_3–SO_4. Stars: spinning side bands, spinning rate 4.7 kHz (top), 4.9 kHz (bottom). Reference: H_3PO_4 85%. Number of accumulations ~3000.

The Lewis acid strength measured from the overall width of the EPR signal of $R^{\ddagger}$ (the aniline radical cation) and the upfield shifted ^{31}P resonances do not match. For the IVB-element oxides, these are between −30 and −33 ppm in spite of a very large difference in their acid strengths. On Al_2O_3–SO_4 which is a weaker Lewis acid than HfO_2–SO_4, the ^{31}P resonance is more upfield shifted, but this may well be a result of the electronic environment of the sites (Al vs IV B elements).

As far as ZrO_2–SO_4 is concerned ^{31}P downfield shifted narrow resonances are observed at +26 and +22.8 ppm on the sample precalcined at 550°C. A weaker line at +22.6 ppm is observed for HfO_2–SO_4, which is almost as strong a Lewis acid as ZrO_2–SO_4. Al_2O_3–SO_4 which comes next in decreasing order of acid strength shows no such downfield shifted line. The +26 and +23 ppm ^{31}P lines in ZrO_2–SO_4 and in HfO_2–SO_4 would correspond to very strong L sites, in agreement with the EPR scaling.

Thus, both Brønsted and Lewis sites are present on the superacids, as it results from

TABLE 1

^{31}P Chemical Shifts (δ_i: ppm with Respect to H_3PO_4 85%), FWHH (kHz) Observed for $(CH_3)_3P$ and w: Difference (gauss) between the Outermost Hyperfine Lines in the EPR Signal of the Aniline Radical Cation

Sample	δ	FWHH	δ	FWHH	δ	FWHH	w
ZrO_2–SO_4	26[b]	0.55	−3.2	0.3	−33	[a]	36.5
	22.8[b]	[a]					
HfO_2–SO_4	22.4	[a]	~−3	0.16	−30	[a]	38.5
Al_2O_3–SO_4			−2.4	0.85	−46.5	2.3	47.7
TiO_2–SO_4			−3.7	1.03[d]	−31	2.3	[c]

[a] Not measurable because of overlapping with SSB, but the simulation indicates a narrower line than for Al_2O_3–SO_4 and TiO_2–SO_4.

[b] In the sample calcined at 650°C, one line (at 26 ppm) only is observable. In the sample calcined at 550°C, two lines at 26 and 22.8 ppm can be separated from SSB.

[c] No hyperfine splitting; hence, w is not measurable.

[d] This line is observed for the sample calcined at 350°C only.

the observation of the infrared spectra of absorbed pyridine and a configuration as that depicted below may account for both types of acid sites (*13*).

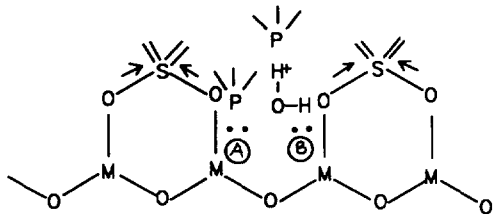

The electron density on a metal center, M, should be lower (and its Lewis acid strength should be higher): (i) for *d* metals with decreasing electronegativity (within the series Ti, Zr, Hf) than for Al, and (ii) at locations on the surface with higher density in electron-withdrawing centers SO_4.

Thus, downfield shifted lines could result from the most electron-deficient metal centers, while the line either near −30 ppm (on the *d* metals) or at −46.5 on Al_2O_3–SO_4 would be attributable to centers more remote from SO_4 groups. Exchange could exist between the A and B configurations depicted above or between an SOH acid group and a nearby TMP:L. In such a case, the two lines corresponding to situations A and B would collapse in a broader one (*15*). As shown later, this possibility seems to be ruled out.

In conclusion of this section, the ranking of the superacids obtained by the sulfate activation $ZrO_2 > HfO_2 > Al_2O_3 > TiO_2$ is a consequence of the nature of the oxide, of the sulfate groups clustering and of oxygen vacancies. TiO_2 is a good example of oxides in which vacancies are easily created by heating under vacuum (*16*). The main ambiguity of the response of the $P(CH_3)_3$ NMR probe is about the origin of the line between −2 and −4 ppm, in the sense that $TMPH^+$ could be formed on residual SOH or on H_2O chemisorbed on strong Lewis sites.

2. *Scaling the Acid Strength in Zeolites and Aluminas*

The same experimental procedure was used for the catalysts. In some cases the pretreatment includes an exposure to O_2 at 450°C, followed by long outgassing in order to clean the surface from organic residues. Figure 3 shows the ^{31}P spectra of $P(CH_3)_3$ adsorbed on different catalysts. Note that all samples contain a fair amount of pentacoordinated Al, except the unground boehmite. Table 2 shows the ^{31}P isotropic shifts and the FWHH (full width at half-

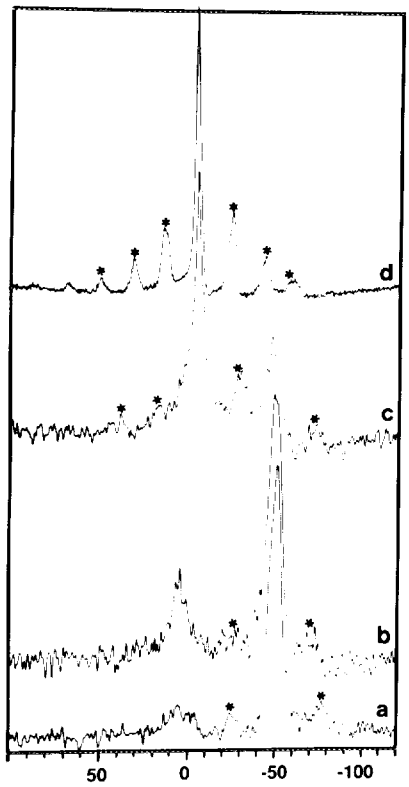

FIG. 3. ^{31}P single-pulse MAS NMR spectrum of TMP chemisorbed on (a) an alumina without observable Al^V, (b) an Al^V-rich alumina; (c) dealuminated, steamed (650) HY; (d) dealuminated mordenite. Conditions similar to those in Fig. 2.

height) of the corresponding lines and the hyperfine splitting constant A_{zz} of O_2^- obtained after first exposing the zeolites to aniline, and aluminas to dimethylaniline, and afterward to O_2 as described earlier (*5*, *14*). The sextet of lines in the g_{zz} tensor of O_2^- indicates that this species interact with Al ($I = 5/2$) and the strength of the corresponding L site should decrease with A_{zz}.

The relative intensities (peak area) of the ^{31}P lines are displayed in Figure 4.

In general, the line between −4 and −8 ppm is accompanied by numerous SSB, while the SSB of the other lines are less intense. A line between −47 and −50 ppm was observed systematically, but we never detected more upfield shifted lines (between −55 and −60 ppm) as did Lunsford and Balthusis, except when the sealed ampule was leaking. We attribute this to the displacement of chemisorbed $P(CH_3)_3$ by atmospheric moisture. The smell is an excellent indicator of imperfect sealing! Sato *et al.* (*17*) have studied TMP chemisorbed on alumina on which silica (from tetraethoxysilane) was vaporized. They have also observed a line at −47 ppm on the bare support and on the support coated with 4.5 wt% silica, in addition to a broad line extending from 10 to −10 ppm. They also reported a line at 28 ppm which appears for SiO_2 coating of 4.5 and 12.3 wt% and not on the bare support or for a SiO_2 loading of 15.7 wt%. They do not comment on that line. As far as we are concerned, we never observed it on our catalysts, except again when we got a leak. They assigned the component of their broad line near 4 ppm to terminal AlOH, because it disappears on samples pretreated above 600°C. Again, except for the alumina rich in Al^V where the line near 5 ppm (Table 2) has a weak intensity, we never detected a line extending from +10 to −10 ppm as reported in Ref. (*17*). In the same vein, Balthusis *et al.* (*10*) have observed a line centered at about −4 ppm on γ-alumina in CP MAS. This line is absent on CP MAS spectra of $(CH_3)_3P$ on γ-alumina described by Lunsford *et al.* (*9*). We underline these discrepancies in order to show how sensitive these systems are with respect to water and O_2. In order to get reproducible results, the outgassing under vacuum (residual pressure $\leq 10^{-5}$ Torr) must be severe and the systems must be absolutely protected from the atmosphere.

The most downfield shifted lines are those observed at −4 ppm on dealuminated mordenite which contains the strongest Lewis acids. The steamed HY (550) which ranks second has a line at −4.8 ppm, and the alumina rich in Al^V which ranks third has a characteristic line at +5 ppm. Note that these lines are broad (1.3 kHz) for the alumina and steamed HY. In the dealuminated mordenite it is narrower (0.8 kHz) and, in addition, a doublet due to J(P–H) coupling has been detected once.

TABLE 2

^{31}P Chemical Shifts (δ_i: ppm with Respect to H_3PO_4 85%), FWHH (kHz) Observed for $(CH_3)_3P$ and A_{zz} (gauss) O_2^- Hyperfine Splitting

Sample	δ	FWHH	δ	FWHH	δ	FWHH	A_{zz}
Dealuminated			−4.3[d]	0.38			
Mordenite			−6.6	—			
			or −4	0.77	−48	1.5	6.3[a]
Steamed HY (550)			−4.8	1.3	−47.2	1.8	5.4
Steamed HY (650)			−8	2.0	−47.3	1.2	n/a
Alumina rich in Al^V (ground boehmite)	5	1.3			−49	1.5	4.9
Alumina poor in Al^V (unground boehmite)		[c]			−50	1.7	[b]
Al_2O_3 (20%)/SiO_2			−4	0.7	−48	1.4	[b]
Calcined HL			−5		−49		5.8[e]

[a] Overall width (w) of the aniline radical cation: 45 gauss, e.g., slightly lower than that on Al_2O_3–SO_4 (see Table 1).

[b] No observable signal.

[c] Very weak line at ~4 ppm.

[d] This doublet has been observed in one case out of two. It is assigned by Lunsford *et al.* (*9*) to a J(P–H) coupling (~0.5 kHz).

[e] w = 48 gauss; see Ref. (*14*).

As said before, our experimental device does not allow CP or ^1H decoupled spectra to be recorded, whereas Lunsford and coworkers have studied very carefully the J(P–H) and the J(P–Al) couplings, which are sources of broadening. Typically, J(P–H) coupling is in the order of 0.5 kHz (see Refs. (*9*) and (*12*), whereas the J(Al–P) coupling is about half this value (*13*).

3. ^{31}P Characteristic NMR Parameters

Low-temperature experiment. If a proton exchange would exist between $TMPH^+$ and TMP:L, the width and position of the ^{31}P MAS lines should change with temperature. Thus, ^{31}P MAS spectra were recorded for TMP adsorbed on the dealuminated mordenite and ZrO_2–SO_4 at temperatures between +25 and −43°C. No measurable differences were observed in either the width or the position of the lines, nor on their relative intensities. These observations rule out the exchange mechanisms. Variable temperature experiments by Lunsford *et al.* (*11*) concluded that an excess $P(CH_3)_3$ is required for initiating the exchange.

^{31}P T_1 measurements. In most of the studied samples, the salient feature is the multiexponential behavior of the magnetization $M(t)$ vs t, in the $(\pi/2, t, \pi/2)$ pulses sequence. If M^* is the magnetization after a "long" time t^* (8s < t^* ≤ 24 s), $M(r)/M^*$ obeys an equation

$$M(t)/M^* = \sum_i P_i[1 - \exp(-t/T_{1i})] \Big/ \sum_i P_i[1 - \exp - (t^*/T_{1i})] \quad (1)$$

with $i > 1$ and where P_i is the population of ^{31}P nuclei with T_{1i} relaxation time, or T_{1i}^{-1} relaxation rate. In such a case there are two possibilities. Either one tries to approximate the spread of T_1^{-1} by an empirical distribution function of T_{1i}. Or, one assumes arbitrarily that $i = 2$ and that there are two fractional ^{31}P populations, P_1 and P_2 with $(P_1 + P_2) = 1$, where P_1 and T_{11} refers to the population relaxing through the paramagnetic impurities, whereas the longer T_{12}, associated with P_2, contains information on the intramolecular and intermolecular con-

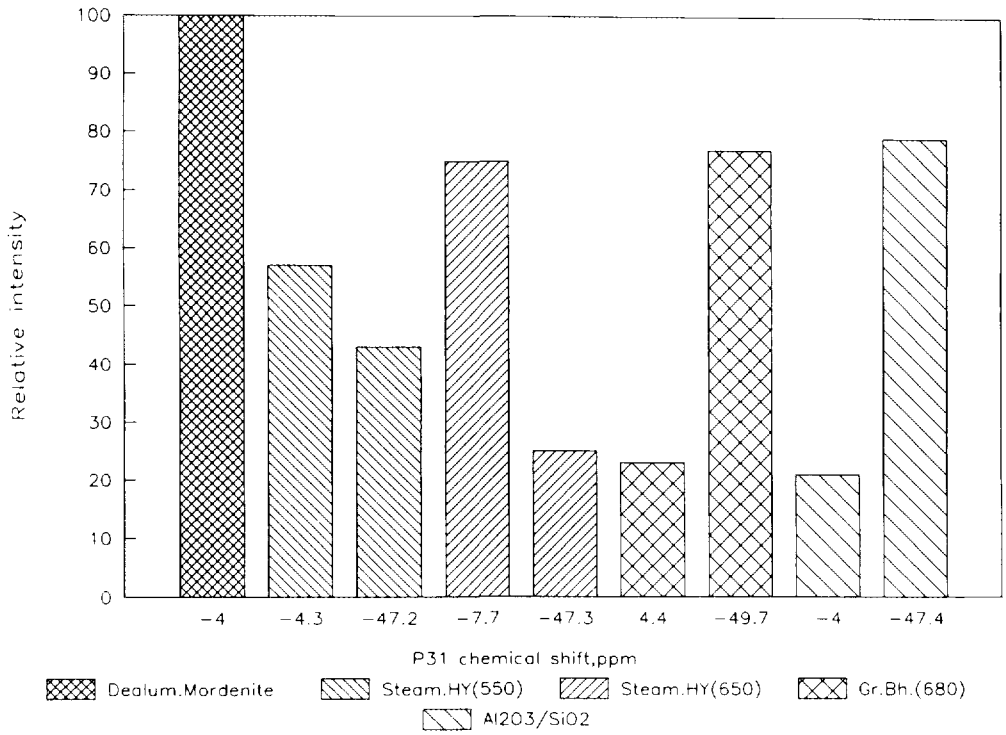

FIG. 4. TMP relative populations in the indicated resonance lines for most of the catalysts reported in Table 2. The alumina GrBh 680 is the Al^{V}-rich alumina. The Al^{V}-poor alumina (Fig. 3a) shows one significant peak only at ~ -50 ppm. The relative populations were obtained from the simulations.

tributions to relaxation. Since it is this kind of information which is relevant to this study, we have chosen that solution. One has to be conscious of the fact that it is a first approximation. Let us remember that (*20*)

$$T_1^{-1} = T_{1\,\text{intra}}^{-1} + T_{1\,\text{inter}}^{-1} + T_{1\,\text{para}}^{-1}. \qquad (2)$$

Thus, T_{11}^{-1} would be dominated by $T_{1\,\text{para}}^{-1}$ whereas T_{12}^{-1} would be essentially $(T_{1\,\text{intra}}^{-1} + T_{1\,\text{inter}}^{-1})$.

In fact, as shown by some examples in Fig. 5 the experimental data can be reasonably fit with two T_1. Table 3 shows the results of this analysis.

As noted before paramagnetic centers have been observed in ZrO_2–SO_4 and HfO_2–SO_4. Steamed HY contains at least four times more Fe^{3+} than dealuminated mordenite, judging from the integrated intensity of the EPR signals at $g \simeq 4$ and $g \simeq 2$. Higher T_{11}^{-1} have been observed in decreasing order in steamed HY, HfO_2–SO_4, and ZrO_2–SO_4, and this observation supports the assignments of T_{11}^{-1} to the relaxation through paramagnetic centers. Note also that dealuminated mordenite is the only sample in which the magnetization recovery is apparently monoexponential ($i = 1$, in Eq. (1)). This zeolite is also the only one which was dealuminated by acid leaching.

Hence, in the following we will assume that T_{12}^{-1} is the sum of the intra and inter contribution as a first approximation. If it is so, the following observations could be predicted. (i) T_{12}^{-1} must be larger for $TMPH^+$ than for TMP for comparable intercontribution. Indeed, the proximity of the extra proton near the phosphorus nucleus must markedly increase the intracontribution. (ii) T_{12}^{-1}

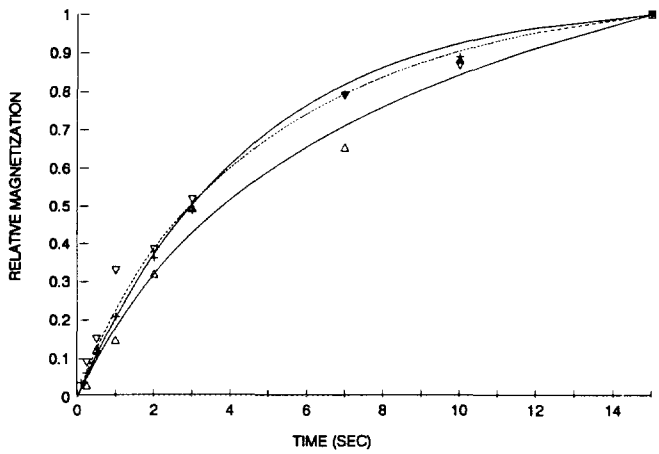

FIG. 5. ^{31}P magnetization recovery $M(t)/M^*$ vs time (s) measured for dealuminated mordenite (+) and ZrO_2–SO_4, ('▽) line at −3.3 ppm and (Δ) line at +26 ppm. The top and bottom solid lines are obtained from Eq. (1) for ZrO_2–SO_4, while the dashed line is that obtained for the dealuminated mordenite (only one population). See the numerical results in Table 3.

must be lower for these species (either TMP or $TMPH^+$) which have restricted rotational/diffusional mobility, that is, for those which are the most strongly adsorbed. Both these predications are verified by the data in Table 3. The lowest T_{12}^{-1} (0.065 s^{-1}) is observed for TMP adsorbed on the strongest Lewis sites in ZrO_2–SO_4. The T_{12}^{-1} values observed for $TMPH^+$ are larger than the corresponding ones observed for TMP adsorbed on the weaker Lewis sites (lines ca. −30 ppm for superacids and ca. −48 ppm for zeolites). Except for both $TMPH^+$ and TMP in steamed HY (650), the average T_{12}^{-1} for $TMPH^+$ is 0.17 ± 0.01 s^{-1} in all the other samples but for the dealuminated mordenite where it is slightly larger (0.22 s^{-1}). The average T_{12}^{-1} for TMP on weaker Lewis sites is 0.13 ± 0.02 s^{-1}. On the steamed HY (650), T_{12}^{-1} is much larger for both $TMPH^+$ and TMP. It might be that because of the abundance of paramagnetic species in this sample, the arbitrary assumption that $i = 2$ in Eq. (1) is too far-fetched.

Thus, the results of the relaxation times measurements contain interesting information. If, as suggested above, the mobility of TMP chemisorbed on strong Lewis sites is negligible, the intramolecular contribution to T_{12}^{-1} is about 0.06 s^{-1}. Therefore, on weaker Lewis sites, the intermolecular contribution is in the same range, namely ~0.07 s^{-1}. The contribution of the extra proton to the intramolecular contribution in $TMPH^+$ should be larger than that of the methyl groups in TMP. Therefore, the values observed for $TMPH^+$ (between 0.17 and 0.22 s^{-1}) is relatively small and it suggests a reduced intermolecular contribution for this species. Another possibility would be that the proton in $TMPH^+$ is, in fact, in rapid exchange between the acidic OH and TMP, and, therefore, that its time-averaged position is not that close to the phosphorus. Measurements of T_1^{-1} vs temperature would be appropriate and they will be carried out in the future.

Chemical shift anisotropy (CSA). If the SSB lines of one transition are well separated from those of another transition, the SSB intensity distribution permits one to obtain the chemical shift tensor through simulation of the distribution. CSA is defined through the principal elements of the tensor according to the equation

$$\text{CSA} = \delta_{33} - (\delta_{11} + \delta_{22})/2,$$

while the asymmetry parameter is $(\delta_{11} +$

TABLE 3

Chemical Shift δ (ppm), Relaxation Rate T_{1i}^{-1} (s^{-1}) and Fractional Population P_i of ^{31}P with that Relaxation Rate, i Is Either 1 or 2 for the Fastest or Lowest Relaxation Rates, Respectively; CSA: Chemical Shift Anisotrophy (kHz)

Sample	δ	T_{1i}^{-1}	P_i	δ	T_{1i}^{-1}	P_i	CSA	δ	T_{1i}^{-1}	P_i	Remarks
ZrO_2–SO_4	26	0.4	0.25	−3.3	0.75	0.15	10.1	−33	*a*	*a*	*a*: Not measurable because of overlapping with SSB
		0.065	0.75		0.17	0.85					
HfO_2–SO_4	22.4	*a*	*a*	−3.5	1.05	0.35		−29	1.3	0.35	*a*: Same remark as above
					0.16	0.65			0.13	0.65	
TiO_2–SO_4				−3.75	0.9	0.27		−30	0.6	0.3	The line at −3.75 ppm is observable in a sample calcined at 350°C.
					0.17	0.73			0.15	0.7	
Dealuminated Mordenite				−4	0.22	1	7.9	−48	*b*	*b*	*b*: The line at −48 ppm is weak and partially overlapped with SSB.
Steamed HY (650)				−8	16.7	0.85	3.4	−47.3	10	0.53	
					1	0.15			0.45	0.47	
Calcined HL				−5	0.9	0.6		−49	0.6	0.55	Sample described in Ref. (5)
					0.18	0.4			0.11	0.45	

TABLE 4

Comparison between the Lewis Acid Strength Scale Obtained from the EPR Measurements and the ^{31}P Chemical Shift. w: Overall Width of the Organic Radical Cation (gauss) or A_{zz}; O_2^- Hyperfine Splitting (gauss)

Sample	w	A_{zz}	Most downfield shifted ^{31}P resonance (ppm)	Most upfield shifted ^{31}P resonance (ppm)
ZrO_2–SO_4	36.5	n.o.[a]	26, 22.8	−33
HfO_2–SO_4	38.5	n.o.	22.4	−30
Dealuminated HM	45	6.3	−4.0	−48
Al_2O_3–SO_4	47.7	n.o.	−2.4	−46.5
Calcined HL	48	5.8	−5	−49
Steamed HY (550)	—[b]	5.4	−4.8	−47.3
Alumina rich in Al^V	—[c]	4.9	5	−49

Note. The strength for TiO_2–SO_4 cannot be estimated because no hyperfine structure of $R^{\cdot}$ is observed.

[a] n.o. means not observable.

[b] No $R^{\cdot}$ observable in absence of O_2.

[c] Dimethylaniline radical cation observable, but the line width is not comparable with that of aniline used for the other sample (see Ref. (*14*)).

$\delta_{22})/(\delta_{33} - \delta_{iso})$, where δ_{iso} is the isotropic chemical shift δ (in Tables 1 and 2).

It has been possible to obtain CSA for the line circa −4 ppm in a few cases, when there was no overlap between sets of SSB. These CSA are shown in Table 3. The asymmetry parameter is close to unity. As it can be observed CSA decreases with increasing T_{12}^{-1} or with increasing intercontribution. The chemical shift anisotropy measures the strength of the indirect coupling between the ^{31}P nucleus and the magnetic field acting on the electrons surrounding the nucleus. It may be expected that an increased mobility of $TMPH^+$ would decrease CSA, in averaging the indirect coupling.

Conclusions of the NMR study. Variable temperature experiments rule out an exchange mechanism such as TMP:L $\underset{H^+}{\rightleftharpoons}$ $TMPH^+$, but T_1 measurements show large differences in the sum of the inter and intra contribution to the relaxation rate (T_{12}^{-1}), for both $TMPH^+$ and TMP:L, on different surfaces. However, because of the multiexponential behavior of the saturation recovery with the time between $\pi/2$ pulses, T_{12}^{-1} is no more than an estimate of the sum of the inter and intracontributions. It seems that the tighter the bond between TMP and Lewis sites is, the lower the intermolecular contribution to T_{12}^{-1}. It has also been suggested that the mobility of $TMPH^+$ is reduced with respect to that of TMP on weak Lewis sites or that the proton in $TMPH^+$ could be shared with the adjacent O^-. In a few cases where measurements of CSA were possible, there seemed to be an inverse relation between CSA and the relaxation rate, not attributable to paramagnetic impurities, that is T_{12}^{-1}.

GENERAL CONCLUSIONS

The scale of the Lewis acid strength obtained from the EPR measurements is summarized in Table 4. If this scale is compared to the results of the ^{31}P MAS NMR measurements reported in Tables 1–3, a positive and a negative conclusion emerge:

(i) Downfield shifted lines are observed in ZrO_2–SO_4 and HfO_2–SO_4, namely, for the strongest Lewis acid, and a line is observed at 5 ppm on Al^V-rich alumina.

(ii) There is no relationship between the position of the upfield shifted line ca. −30 ppm in the superacids or ca. −48 ppm in Al_2O_3–SO_4, in aluminas, or in zeolites and the Lewis acid strength.

Then the question is: Which ^{31}P resonance

has to be assigned to the strong Lewis sites in zeolites? Unless their surface density is very small and/or unless their observation is impossible because of the overlapping of the SSB of the other lines, a possible answer is that these strong Lewis sites are blocked by chemisorbed water which would not be removed at 450°C in vacuum before the contact with TMP and that they would form $TMPH^+$. A complete water removal seems improbable, since the same pretreatment uncovers strong Lewis sites in the superacids. It might be that the strong L sites in zeolites are in the proximity of Brønsted sites and that the observed $TMPH^+$ species results from the interaction between both kinds of sites. The L sites would weaken the electron density in the oxygen of the acidic OH. Then one wonders why these L sites would contribute to the formation of the aniline radical cation.

Thus, the information obtained from the EPR and NMR molecular probes, with respect to the scaling of the Lewis acid strength, converge on the existence of very strong Lewis sites, such as in ZrO_2–SO_4 or HfO_2–SO_4. TMP reveals relatively weak Lewis acid centers, but apparently fails to show stronger Lewis sites in zeolites, unless the formation of $TMPH^+$ results partially from synergy between Brønsted sites and these strong Lewis sites.

ACKNOWLEDGMENTS

This work has been made possible by DOE Grant DE-FG02-90 ER1430.

REFERENCES

1. Umansky, B., and Hall, W. K., *J. Catal.* **124,** 97 (1990), and references therein.
2. Stamires, D. N., and Turkevich, J., *J. Am. Chem. Soc.* **85,** 2557 (1963).
3. Hall, W. K., *J. Catal.* **1,** 53 (1962), and references therein.
4. Chen, F. R., and Fripiat, J. J., *J. Phys. Chem.* **96,** 819 (1992).
5. Chen, F. R., and Fripiat, J. J., *in* "Proceedings, 9th International Conference on Zeolites, Montreal, July 1992," in press.
6. Ayscouph, P. B., "Electron Spin Resonance in Chemistry," p. 6. Methuen and Co., London, 1967.
7. Chen, F. R., and Guo, X. X., *J. Chem. Soc. Chem. Commun.* **1** 1682 (1989).
8. Rothwell, W. P., Shen., W. X., Lunsford, J. H., *J. Am. Chem. Soc.* **106,** 2452 (1984).
9. Lunsford, J. H., Rothwell, W. P., and Shen, W. X., *J. Am. Chem. Soc.* **107,** 1540 (1985).
10. Balthusis, L., Frye, J. S., and Maciel, G. E., *J. Am. Chem. Soc.* **108,** 7119 (1986); **109,** 40 (1987).
11. Lunsford, J. H., Tuntunjian, P. N., Chu, P. J., Yeh, E. B., and Zalewski, D. J., *J. Phys. Chem.* **93,** 2590 (1989).
12. Chu, P. J., de Mallman, A., and Lunsford, J. H., *J. Phys. Chem.* **95,** 7362 (1991).
13. Arata, K., *Adv. Catal.* **37,** 165 (1990), and references therein.
14. Chen, F. R., Davis, J. G., and Fripiat, J. J., *J. Catal.* **133,** 263 (1992).
15. Gutowsky, H. S., and Saika, A., *J. Chem. Phys.* **21,** 1688 (1953).
16. Vannice, M. A., Odier, P., Bujor, M., and Fripiat, J. J., *ACS Symposium Series No. 288 Catalyst Characterization Science* (M. L. Denny, and J. L. Gland, Eds.), 9, 1985.
17. Sato, S., Sodesawa, T., Nozaki, F., and Shoji, H., *J. Molec. Cataly.* **66,** 343 (1991).
18. Chen, F. R., Cheng, S., Zong, W., Guo, X., and Fripiat, J. J., *J. Chem. Soc. Faraday Trans.*, **88,** 887 (1992).
19. Hong, Y., Coster, D. J., Chen, F. R., Davis, J. G., and Fripiat, J. J., *in* "Proceedings, 10th International Congress on Catalysis, Budapest, Hungary, 1992," in press.
20. Abragham, A., "Les Principes du Magnétisme Nucléaire," p. 308 and following. Presses Universitaires de France, 1961.